

## Correlation in laser speckle

J. H. Li and A. Z. Genack

*Department of Physics, Queens College of The City University of New York, Flushing, New York 11367*

(Received 16 December 1993)

We demonstrate experimentally that the intensity correlation function with shift in the scattered wave vector or with identical shifts in both the incident and scattered wave vectors form Fourier transform pairs, respectively, with the intensity distribution on the output surface and the propagator between the input and output surfaces. Measurements in samples with and without internal reflection are in excellent agreement with diffusion theory without adjustable parameters.

PACS number(s): 42.25.Bs, 42.25.Fx, 42.30.Ms

The nature of wave propagation in random media is revealed in the degree of correlation of intensity fluctuations as a function of the spatial, spectral, or temporal parameters of the incident or scattered wave [1]. Perhaps the most dramatic display of wave correlation is the grainy appearance of the scattered laser light known as laser speckle [2]. Nonetheless, a quantitative study of the angular correlation within the static speckle pattern of transmitted multiply scattered light and its relationship to the underlying diffusion within the medium and to other correlation functions involving shifts in both the incident and scattered wave vectors has not been presented previously. The intensity correlation function which has been investigated most extensively is the "memory effect," in which both the incident and scattered wave vector are shifted by the same amount [3–7]. In this case, the output speckle pattern appears to track changes in the incident wave vector and the range of wave vector change over which correlation persists is therefore considerably larger than that which is found within the speckle pattern for fixed incident excitation. Freund, Rosenbluh, and Feng [4] found a discrepancy between measurements of the memory effect and calculations by Feng, Kane, Lee, and Stone [3]. They showed [6] that this discrepancy could be largely removed by incorporating internal reflection [8] in the description of transport and using the internal reflection coefficient  $R$  in the expression for the memory effect as a fitting parameter. In this paper, we confirm experimentally an expression for intensity correlation as a function of arbitrary shift in the incident and scattered wave vectors in terms of surface intensity distributions. Measurements of the angular intensity correlation function within the static speckle pattern and the memory effect are shown to be Fourier transforms, respectively, of measurements of the intensity distribution on the output surface and of the propagator between the input and output surfaces which is the output spatial intensity distribution for a tightly focused incident beam. These results are consistent with diffusion theory using a value for  $R$  which is found independently from measurements of the scale dependence of transmission [9].

Intensity correlation has generally been considered in a waveguide geometry between the  $N = Ak^2/2\pi$  distinct

transverse momentum and polarization channels of a waveguide of area  $A$  at frequency  $\omega = ck$  [3,10]. The transmission coefficient from channel  $a$  on the left of the disordered region to channel  $b$  on the right is denoted as  $T_{ba}$ . Macroscopic matrix [10] and diagrammatic [3] calculations show that the correlation matrix  $C_{ab,a'b'} = \langle \delta T_{ba} \delta T_{b'a'} \rangle$  of fractional fluctuations in the transmission coefficients from their ensemble average values  $\delta T_{ba} = (T_{ba} - \langle T_{ba} \rangle) / \langle T_{ba} \rangle$  can then be written as a sum of three terms distinguished by the range of correlation between modes [3,10],

$$C_{ab,a'b'} = C_{ab,a'b'}^{(1)} + C_{ab,a'b'}^{(2)} + C_{ab,a'b'}^{(3)}. \quad (1)$$

When the sample length  $L$  within the waveguide is much greater than its width  $W \sim A^{1/2}$ , the ensemble average of the intensity distribution in the transverse coordinate has a width  $W$  independent of the distribution of the incident excitation. The correlation matrix may then be written as [10]

$$C_{ab,a'b'} = A_1 \delta_{aa'} \delta_{bb'} + A_2 (\delta_{aa'} + \delta_{bb'}) + A_3. \quad (2)$$

The coefficients  $A_1$ ,  $A_2$ , and  $A_3$  are of order 1,  $1/g$ , and  $1/g^2$  respectively, where  $g$  is the dimensionless conductance  $g \sim Nl/L$ , and where  $l$  is the photon transport mean free path. The first term arises in the field factorization approximation,  $C_{ab,a'b'}^{(1)} = |I_{ab,a'b'}|^2$ , where  $I_{ab,a'b'} = \langle \mathbf{E}_{ab} \cdot \mathbf{E}_{a'b'}^* \rangle$ , and  $\langle \dots \rangle$  denotes an average over an ensemble of sample configurations [11]. This term dominates intensity fluctuations. The Kronecker  $\delta$  in the  $C_1$  term represents the sharp cutoff of correlation between different transverse momentum channels with a correlation wave vector of  $\delta k \sim 1/W$ . The  $C_2$  term gives rise to long-range correlation and dominates transmission fluctuations, whereas the  $C_3$  term is the source of universal conductance fluctuations. Only the lowest order  $C_1$  term will be discussed here.

For a slab geometry illuminated by a wide beam such that the width of the output intensity distribution is much greater than the slab thickness,  $\delta\rho \gg L$ , Feng *et al.* found [3]

$$C_{k_a k_b k'_a k'_b}^{(1)} = A_1 \delta_{\Delta K_a, \Delta k_b} F_1(\Delta k_a L), \quad (3)$$

where

$$F_1(x) = x^2 / \sinh^2 x. \quad (4)$$

The Kronecker  $\delta$  in shifts  $\Delta \mathbf{k}_a$  and  $\Delta \mathbf{k}_b$  of the incident and scattered wave vectors, respectively, reflects the short correlation range  $\delta k \sim 1/\delta\rho$  when either the incident or scattered wave vector is changed separately. On the other hand, the range of the correlation function  $F_1(\Delta k_a L)$  for identical shifts in the incident and scattered wave vectors is  $\delta k \sim 1/L$ . The function  $F_1$  is found to be the Fourier transform of the intensity propagator between the input and output surfaces [6]. This result is analogous to the intensity correlator with frequency shift [12] in which the input and detected frequency are shifted by the same amount. The intensity correlation function with frequency shift then becomes the Fourier transform of the time-of-flight distribution across the slab, which is the propagator in the time domain [13].

The field correlation function  $I_{\{k_a\}k_b, \{k'_a\}k'_b}$  between a field  $E_{\{k_a\}k_b}$  with scattered wave vector  $\mathbf{k}_b$  arising from a distribution of incident wave vectors represented by  $\{\mathbf{k}_a\}$ , which give rise to an intensity distribution  $I(\rho_a)$  in the transverse coordinate  $\rho_a$  on the incident surface and a field  $E_{\{k'_a\}k'_b}$ , can be written as [6,14]

$$I_{\{k_a\}k_b, \{k'_a\}k'_b} \propto \iint I(\rho_a) P(\rho_b - \rho_a) \times \exp[i(\Delta \mathbf{k}_a \cdot \rho_a - \Delta \mathbf{k}_b \cdot \rho_b)] d\rho_a d\rho_b, \quad (5)$$

where  $P(\rho_b - \rho_a)$  is the intensity propagator in the transverse displacement between the output and input surfaces. For  $g \gg 1$ , the intensity correlation function is the amplitude square of the field correlation function.

In this paper, we verify Eq. (5) experimentally in two special cases. For the first case in which  $\Delta \mathbf{k}_a = 0$ , Eq. (5) is integrated over  $\rho_a$  and squared to give the correlation function,

$$C(\Delta \mathbf{k}_b) \propto \left| \int I(\rho_b) \exp(-i \Delta \mathbf{k}_b \cdot \rho_b) d\rho_b \right|^2, \quad \Delta \mathbf{k}_a = 0, \quad (6)$$

where  $I(\rho_b) = \int I(\rho_a) P(\rho_b - \rho_a) d\rho_a$  is the intensity distribution on the output surface given by the convolution of the input intensity distribution with the propagator. Equation (6) shows that the field correlation function versus  $\Delta \mathbf{k}_b$  and the intensity distribution as a function of  $\rho_b$  are a Fourier transform pair. Consequently, if  $\delta\rho$  is the width of  $I(\rho_b)$ , the range of correlation in the static speckle pattern is  $\delta k \sim 1/\delta\rho$ . Equation (6) is also a manifestation of the van Cittert-Zernike theorem of classical coherence theory which gives a spatial correlation along a screen for light emitted by an incoherent planar source [15].

For the second case, in which  $\Delta \mathbf{k}_a = \Delta \mathbf{k}_b \equiv \Delta \mathbf{k}$ , we obtain the intensity correlation function

$$C(\Delta \mathbf{k}) \propto \left| \int P(\rho) \exp(-i \Delta \mathbf{k} \cdot \rho) d\rho \right|^2, \quad \Delta \mathbf{k}_a = \Delta \mathbf{k}_b \quad (7)$$

(internal reflection). It shows that the intensity correla-

tion function, with  $\Delta \mathbf{k}$ , is the amplitude square of the Fourier transform, and  $P(\rho)$ , where  $\rho = \rho_b - \rho_a$ . Since the width of  $P(\rho)$  is  $\delta\rho_0 \sim L$ , the range of the correlation  $\delta k \sim 1/L$ .

The relationships (6) and (7) between intensity correlation functions and intensity distributions are explicitly confirmed in measurements of these quantities made on a 280- $\mu\text{m}$  polycrystalline alumina slab. The sample provided by Valley Design Corporation is 99.7% alumina with a solid fraction of 0.97. From the measured specular reflection coefficient 0.072 near normal incidence with a He-Ne laser, we find the refractive index of the sample to be 1.70, which is close to the refractive index 1.76 of pure alumina. From measurements of total transmission versus thickness in a wedge, we find that the transport mean free path in this material is  $l = 31.4 \mu\text{m}$  and the internal reflection coefficient  $R = 0.81$  [9]. Since the sum of reflected and transmitted light in this sample is equal to the incident intensity within the experimental uncertainty of 1%, absorption is negligible.

In the present experiments a 3-mW He-Ne laser beam is expanded, collimated, and then focused on the sample surface. The sample is mounted on the center of a goniometer. Intensity spectra in the far field as a function of the angle of the detector with respect to the normal of the fixed sample are recorded by sweeping the detector along an arc from  $-1.5^\circ$  to  $1.5^\circ$ . The normalized intensity correlation function versus shift  $\Delta\theta$  in the angle of the detector,  $C(\Delta\theta) = \langle \delta I(\theta) \delta I(\theta + \Delta\theta) \rangle$ , was computed from 100 such intensity spectra recorded by illuminating different areas of the sample. Correlation functions are calculated using intensity spectra normalized by the angular intensity distribution  $\langle I(\theta) \rangle$  obtained from the average of all spectra. We have also recorded intensity spectra as a function of the rotation angle of the sample with respect to the fixed detector in the forward direction. The total rotation of the sample is about  $3^\circ$ . These measurements were made for broad and narrow incident beams. Measurements are made for the sample immersed in index-matching fluid as well as in air. The

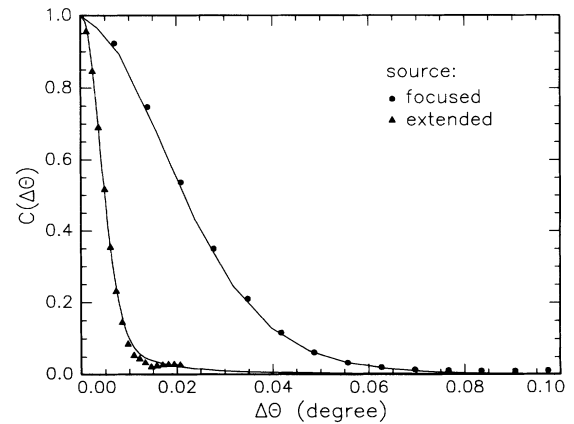


FIG. 1. Intensity correlation functions  $C(\Delta\theta)$  vs detector angle for an alumina sample in air for laser beams focused on 5  $\mu\text{m}$  and 2 mm. The solid lines are the Fourier transforms of the intensity profiles for focused and wide beams, respectively. The data shown in figures are for  $L = 280 \mu\text{m}$ .

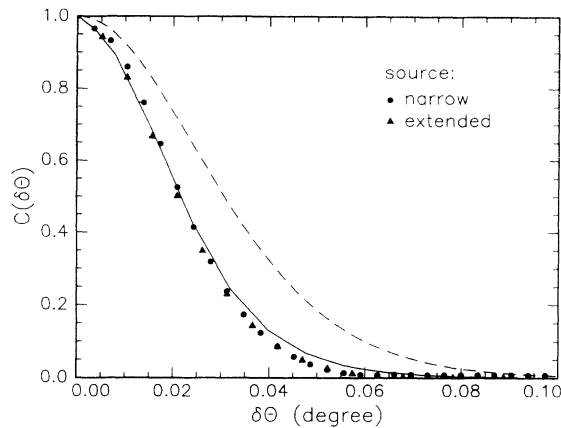


FIG. 2. Intensity correlation functions  $C(\delta\theta)$  vs rotation angle of the sample in air for laser beams focused to  $50\ \mu\text{m}$  and expanded to  $2\ \text{mm}$ , respectively. The solid line is the same as in Fig. 1. The dashed line is  $F_1$  in Eq. (4).

cumulant intensity correlation function versus shift  $\delta\theta$  in the sample rotation angle,  $C(\delta\theta) = \langle \delta I(\theta)\delta I(\theta + \delta\theta) \rangle$ , was calculated using 100 intensity spectra normalized by the average of all intensity spectra.

The intensity correlation functions versus detector angle  $C(\Delta\theta)$  for an incident beam focused to a  $5\text{-}\mu\text{m}$ -diam spot and for a beam expanded to a spot  $2.0\ \text{mm}$  in diameter on the alumina sample in air are shown as the dots and triangles in Fig. 1. The narrower the intensity distribution, the broader the corresponding angular correlation function. The solid lines are the amplitude square of the Fourier transform of the surface intensity distribution  $I(\rho_b)$  measured for the focused and broad beams. The agreement with the corresponding correlation functions confirms Eq. (6).

The angular correlation function  $C(\delta\theta)$  measured for the sample in air is shown in Fig. 2. The dots give the measured intensity correlation function with sample rotation angle  $\delta\theta$  using a laser beam focused to  $50\ \mu\text{m}$ . The triangles give the same correlation function for a  $2\text{-mm}$ -diam incident beam. These results show that  $C(\delta\theta)$  is independent of the incident beam profile [4] in accord with Eq. (7). The solid line shown in Fig. 2, which gives the amplitude square of the Fourier transform of the intensity profile for a tightly focused spot, is reproduced from Fig. 1. The agreement with both sets of data confirms Eq. (7) since  $I(\rho_b)$  for the focused beam is the diffusion propagator  $P(\rho)$ . The measurement of  $I(\rho_b)$  for the focused beam is in excellent agreement with calculations of the diffusion theory using scattering parameters measured for this sample [9]. This confirms that these measurements of angular correlation are consistent with diffusion theory. The correlation function given by Eq. (4), which does not include the influence of internal

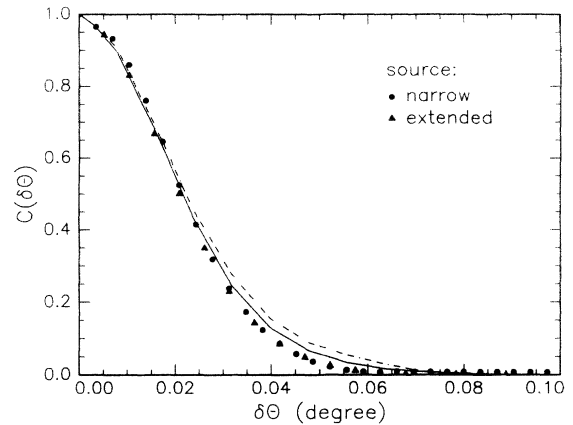


FIG. 3. Intensity correlation function vs rotation angle of the sample immersed in index matching fluid for incident beam diameters of  $50\ \mu\text{m}$ . The solid line is the square amplitude of the Fourier transform of the calculated diffusion propagator and the dashed line is given by Eq. (4).

reflection, is shown as the dashed line in Fig. 2.

The role of internal reflection is further considered in the measurements of the angular correlation function  $C(\delta\theta)$  for the sample immersed in index matching fluid with  $n=1.70$  for an incident beam focused to a  $50\text{-}\mu\text{m}$  spot. This correlation function, shown in Fig. 3, is broader than that for the sample in air because the surface propagator is narrower. The solid line is the amplitude square of the Fourier transform of the calculated diffusion propagator with  $R=0$  using the propagation parameters given above. This line is also in excellent agreement with Eq. (7), using the intensity profile measured for a tightly focused beam. The dashed line is the angular form factor  $F_1$  given in Eq. (4). The agreement demonstrates that the calculations of Feng *et al.* accurately describe the “memory effect” in the absence of internal reflection.

In conclusion, we have confirmed a general expression for angular correlation functions with arbitrary shift in incident and scattered wave vectors in the field factorization approximation in a study of angular correlation within the static speckle pattern and the memory effect. We demonstrate that the angular intensity correlation function in transmission is fully described by the photon diffusion model when internal reflection is taken into account.

We thank A. A. Lisiansky for stimulating discussions and for valuable comments on the manuscript. This work was supported by the NSF under Grant No. DMR-9001335, by the Petroleum Research Fund of the ACS under Grant No. 22800-AC, 7, and by PSC-CUNY.

[1] *The Scattering and Localization of Classical Waves*, edited by P. Sheng (World Scientific, Singapore, 1990).

[2] *Laser Speckle and Related Phenomena, Topics in Applied Physics*, edited by J. C. Dainty (Springer-Verlag, Berlin,

1984), Vol. 9.

[3] S. Feng, C. Kane, P. A. Lee, and A. D. Stone, *Phys. Rev. Lett.* **61**, 834 (1988).

[4] I. Freund, M. Rosenbluh, and S. Feng, *Phys. Rev. Lett.*

- 61, 2328 (1988).
- [5] I. Freund and R. Berkovits, *Phys. Rev. B* **41**, 496 (1990).
- [6] R. Berkovits, M. Kaveh, and S. Feng, *Phys. Rev. B* **40**, 737 (1989).
- [7] J. X. Zhu, D. J. Pine, and D. A. Weitz, *Phys. Rev. A* **44**, 3948 (1991).
- [8] A. Lagendijk, R. Vreeker, and P. de Vries, *Phys. Lett. A* **136**, 81 (1989).
- [9] J. H. Li, A. A. Lisyansky, T. D. Cheung, D. Livdan, and A. Z. Genack, *Europhys. Lett.* **22**, 675 (1993).
- [10] P. A. Mello, *Phys. Rev. Lett.* **60**, 1089 (1988); P. A. Mello, E. Akkermans, and B. Shapiro, *ibid.* **61**, 459 (1988).
- [11] B. Shapiro, *Phys. Rev. Lett.* **57**, 2168 (1986).
- [12] A. Z. Genack, *Phys. Rev. Lett.* **58**, 2043 (1987).
- [13] A. Z. Genack and J. M. Drake, *Europhys. Lett.* **11**, 331 (1990).
- [14] A. Z. Genack, J. H. Li, N. Garcia, and A. A. Lisyansky, in *Photonic Band Gaps and Localization*, edited by C. M. Soukoulis (Plenum, New York, 1993).
- [15] M. Born and E. Wolf, in *Principles of Optics*, 4th ed. (Pergamon, New York, 1970), p. 508.